

# ON COMPUTER-AIDED FRACTAL ANALYSIS OF GROWTH PROCESSES AT TUMOR-STROMA BORDER

MIHAI TANASE

*Politehnica University of Bucharest  
Splaiul Independentei 313, Bucuresti, Romania  
E-mail: tanase2009@yahoo.com*

**Abstract.** In the characterization of carcinomas, an important criterion is the shape of the tumor-stroma frontier and, in particular, its fractal dimension. The definition and identification of this frontier is not trivial. For the same image, the known segmentation algorithms often produce frontiers with very different fractal dimensions making this type of analysis irrelevant. We introduce a new approach to frontier analysis by redefining the tumor-stroma frontier in order to overcome this problem.

**1. Introduction.** Segmentation is in general defined as the process of partitioning an image such that the pixels of each of the parts are logically related. In particular this translates in partitioning the image such that each pixel is assigned to an object. In medical imaging, the segmentation means the identification of tissues. By segmentation we understand the procedure that extracts from the image the maximal connected sets of pixels that belong to the representation of a single tissue. These sets are called segments. Many general segmentation algorithms have been proposed including the Region-Growing algorithms [9, 2].

The micro-environment plays a decisive role in tumor growth. The interaction between the tumor cells and the stroma cells is essential for tumor growth and metastasis and it is precisely the factor which generates the shape of the tumor-stroma frontier [10, 4, 15, 1, 3, 13].

---

2010 *Mathematics Subject Classification:* Primary 68-XX; Secondary 68T45.

*Key words and phrases:* tumor-stroma border, fractal dimension, segmentation algorithm, frontier-band.

The content of this paper is mainly a presentation of parts of the work developed by the author in [12] related to the title.

The paper is in final form and no version of it will be published elsewhere.

In the characterization of carcinomas, an important criterion is the shape of the tumor-stroma frontier and, in particular, its fractal dimension [14, 11]. But the fractal dimension of the frontier strongly depends on how the frontier was defined in the first place. In the case of macroscopic medical images, there is no rigorous general accepted way to define the frontier. More precisely, for the same image, each segmentation algorithm may produce a different frontier with a different fractal dimension.

This variation can be wide enough to make the results of the analysis be more of a characterization of the segmentation algorithm rather than a characterization of the tumor itself. Thus, this problem is both a conceptual and a technical one (see Fig. 1, Fig. 2).

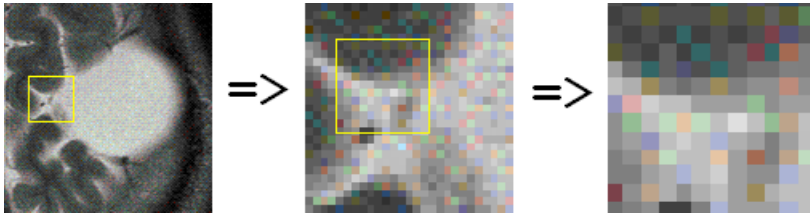


Fig. 1. The contour of the tumor in the image is hard to define at the pixel level

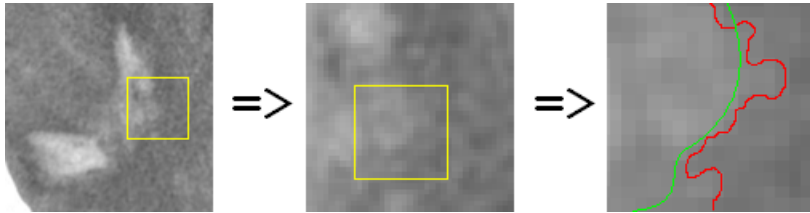


Fig. 2. Both contours (green or red) are equally valid while no rigorous and relevant criteria are defined. However, they have completely different fractal dimensions

In the usual approach to this problem, the frontier is first determined by using some segmentation method, then it is extracted (i.e. represented as a contiguous chain of pixels; several efficient algorithms are known for the extraction procedure [7]) and only then its fractal dimension is computed. But in this way, the results of the fractal analysis will be based not only on the criterion of fractal dimension which is a well-defined mathematical notion, but also on the segmentation criteria which are mostly subjective. In the case of tumor-stroma frontier, the subjectivity range is even wider. For example, it is not always appropriate to apply to biological structures a segmentation method that is based on the characterization of the contours of artificial objects like color variation, sharp edges *etc.* The geometry of biological structures in general and of tissues in particular is much more complicated and hard to characterize than the geometry of the artificial structures. Thus, in the case of biological structures we have not only the variation induced by the technical implementation, but also a much more uncontrollable variation induced by the conceptual issues regarding the definition of a frontier.

Many algorithms try to mimic the human perception which is better adapted to a different scale and to different patterns than the ones characterizing biological tissues.

Also, in the case of tumors, we are not dealing with simple curves and sharp edges as in the typical case of artificial objects.

One of key issues with the classical segmentation algorithms is that the analysis on which they are based is ultimately, in some sense, too local.

Each segmentation algorithm preserves and captures particular morphological aspects of the segments and frontiers considered to be relevant by the algorithm. What we need is an algorithm that preserves and captures fractal dimension in the general sense.

We propose a new approach which is based on the following idea: If our ultimate objective criterion is the fractal dimension, we should use the fractal dimension as the basic criterion in the segmentation as well.

More precisely, we shall redefine the notion of frontier between two biological structures. In particular, we shall redefine the notion of tumor-stroma frontier at the macroscopic level.

**2. A new approach to the problem of frontier**

**2.1. Fractal dimension.** The term “fractal dimension” was coined by Mandelbrot in 1975. However, the main ideas of fractal dimensions belong to Hausdorff. While the topological dimension is an integer number, the fractal dimension can be non-integer and this concept is central to the definition of fractals.

DEFINITION 1 ([8]). Let  $\mathbb{R}^n = \{x = (x_1, x_2, \dots, x_n) : x_i \in \mathbb{R}\}$  and let

$$d(x, y) = \sqrt{\sum_{i=1}^n (x_i - y_i)^2} \quad \forall (x, y) \in \mathbb{R}^n \times \mathbb{R}^n$$

be the Euclidean distance. The *diameter* of a subset  $U \subset \mathbb{R}^n$  is defined by

$$\text{diam}(U) = \sup\{d(x, y) : x, y \in U\}.$$

Let  $A \subset \mathbb{R}^n$  and let  $\{U_i, U_2, \dots\}$  be an open cover of  $A$ . For any  $s > 0$  and  $\epsilon > 0$  we define

$$h_\epsilon^s = \inf\left\{\sum_i \text{diam}(U_i)^s\right\}.$$

The  $s$ -dimensional Hausdorff measure of  $A$  is  $h^s(A) = \lim_{\epsilon \rightarrow 0} h_\epsilon^s(A)$ . One can prove that there is a number  $D_H(A)$  such that  $h^s(A) = \infty$  if  $s < D_H(A)$  and  $h^s(A) = 0$  if  $s > D_H(A)$ . The number  $D_H(A)$  is the *Hausdorff dimension* of  $A$  and it can be zero, infinity or a positive real number. Moreover,

$$D_H(A) = \inf\{s : h^s(A) = 0\} = \sup\{s : h^s(A) = \infty\}.$$

Some basic properties of the Hausdorff dimension are:

- (1) if  $A \subset \mathbb{R}^n$  then  $D_H(A) \leq n$ ;
- (2) if  $A \subset B$  then  $D_H(A) \leq D_H(B)$ ;
- (3) if  $A$  is countable then  $D_H(A) = 0$ ;
- (4) if  $D_H(A) < 1$  then  $A$  is totally disconnected.

DEFINITION 2. A set is a *fractal* if its Hausdorff dimension is different from its topological dimension.

For some classical fractals, we can find the Hausdorff dimension simply by evaluating the ratio  $D = \frac{\log(N)}{\log(r)}$ , where  $N$  is the number of smaller parts of the fractal which are copies of the whole and  $r$  is the scaling factor that makes a smaller part as big as the whole. But in the general case, it is difficult to evaluate the Hausdorff dimension of a particular set. An alternative to the Hausdorff dimension is the Minkowski–Bouligand dimension, also called the box-counting dimension, which is easier to compute by the well-known algorithms. These algorithms are based on one particular idea: evaluate the object at different scales and capture the relation between the result of measurement and the scale. For a fractal object this relation is a power law with the exponent being an estimate of the fractal dimension.

The classical box-counting algorithm is used to estimate the fractal dimension of a bounded set of points in the plane. Its adaptation for digital images works only on binary images. For gray-levels images, one can apply the binary version of the algorithm only after applying a filter to the image to obtain a binary one. This is usually done by fixing a threshold on the level of gray. However, this method has two major disadvantages: the lack of rigorous criteria in selecting the threshold and the dramatic loss of information this procedure implies.

In many applications, we are interested in analyzing gray-levels images (e.g. CT or MRI). In general, the gray levels must have a precise interpretation, otherwise the analysis results may be irrelevant. The algorithm below computes a number which we call *textural fractal dimension*. We shall omit the word “textural” for convenience; also, by “square” we understand a square with interior or a “box”.

ALGORITHM ([6]).

- Let  $A$  be a given bounded set of points in the plane and let  $g : A \rightarrow \mathbb{R}$  be a given function which assigns to each point  $p \in A$  a non-negative real value, namely its gray level.
- We extend the definition of  $g$  to the entire plane by letting  $g(p) = 0$  for all  $p \in \mathbb{R} \setminus A$ .
- For a positive number  $r > 0$ , we cover the set  $A$  with squares of size  $r \times r$  such that no two squares overlap. Thus, we obtain a family of squares  $C_r = \{S_1, S_2, \dots, S_{n_r}\}$ . For each square  $S_i$  in the family, let  $G_i = \sup\{g(p) : p \in S_i\}$  and let  $H_i = \lceil \frac{G_i}{r} \rceil$ . Then  $N_r = \sum_{i=1}^{n_r} H_i$ .
- We choose different values for  $r$  to obtain different pairs  $(\log(r), -\log(N_r))$ . In applications, the best results were obtained by choosing  $r \in \{ku, (k-1)u, \dots, 3u, 2u, u\}$  for a fixed natural number  $k > 1$  and a unit  $u$  as one can see in the implementation.
- If we plot the obtained pairs as points on a diagram we can compute the slope of the regression line and denote it by  $\alpha$ . This will be the result of the algorithm and we call it the *textural fractal dimension* of  $(A, g)$ .

## 2.2. The local fractal dimension map

DEFINITION 3. Let  $A$  be a set of points in  $\mathbb{R}^n$ . Let  $c \in \mathbb{R}^n$  be a point in the space and  $\rho$  be a real positive number. We define the *local fractal dimension of  $A$  in  $c$  by radius  $\rho$*  to be the fractal dimension of the subset of points  $A \cap B_\rho(c)$ , where  $B_\rho(c)$  denotes the open ball of radius  $\rho$  and center  $c$ .

In practical application we use the alternative definition given below:

DEFINITION 4. Let  $A$  be a set of points in  $\mathbb{R}^n$ . Let  $c \in \mathbb{R}^n$  be a point in the space and  $\rho$  be a real positive number. We define the *local fractal dimension of  $A$  in  $c$  by radius  $\rho$*  to be the fractal dimension of the subset of points  $A \cap S_\rho(c)$  where  $S_\rho(c)$  is the interior of the cube with edges of length  $2\rho$  and with the center in  $c$ .

In applications, the evaluation of the local fractal dimension of an object represented in an image can be done by first selecting a pixel  $c$  as the center and then computing the fractal dimension of that part of the image which lies inside the square of size  $2\rho \times 2\rho$  centered in  $c$ .

One can make the analogy between the property of usual objects to have a local color with the property of some natural structures to have local fractal dimensions. In fact, while the most of the segmentation algorithms are based on the color of pixels, the algorithm presented here is based on the local fractal dimension of the neighborhoods of pixels.

In many important cases, the analyzed image does not represent a single fractal, but many fractals in contact. In other words, the structure we want to analyze is not homogeneous with respect to the local rule of growth or construction and so with respect to the local fractal dimension, as well as usual objects may also be not homogeneous with respect to their color as a reflection of non-homogeneity of the material.

One of the problems we want to solve is to determine the different homogeneous structures of an object. For instance, in a medical image, one wants to identify the different structures, i.e. tissues represented in the image.

Therefore, what is needed is a way to represent the rules of growth of the local structures as local fractal dimensions on some kind of a map associated to the studied object. We call such a map *the local fractal dimension map* and we present below its mathematical definition.

DEFINITION 5. Let  $A$  be a set of points in  $\mathbb{R}^n$ . We fix a real positive number  $\rho$ . The *local fractal dimension map of  $A$  by radius  $\rho$*  is a non-negative real function  $\Phi_\rho : A \rightarrow \mathbb{R}$  where  $\Phi_\rho(p)$  is the local fractal dimension of  $A$  in  $p$  by radius  $\rho$ .

This definition relies on the choice of the radius  $\rho$ . This is analogous to the “distance” from which we evaluate the object. One can admit that there are no perfectly homogeneous objects in nature — even the most homogeneous ones are heterogeneous at the subatomic level. Therefore when one judges the property of homogeneity of an object, one must agree on a reference scale or resolution. This scale is reflected in the parameter  $\rho$  which tells what is the reference size of the parts which are supposed to be generated by the same rule under the hypothesis of structural homogeneity.

In the following, we present the algorithm for computing the local fractal dimension map in the case of gray-level images.

ALGORITHM ([6]).

- Let  $I$  be a digital gray-levels image representing an object or a group of objects. Let  $w$  be the number of columns and  $h$  be the number of rows of pixels of the image. The columns and rows are indexed from 0.

- Let  $P$  be a fixed palette of colors, i.e. an array of  $(r, g, b)$  triples (red, green, blue) and  $\eta : [0, \infty) \rightarrow P$  be a function that associates a color to each non-negative real number.
- We fix the radius  $\rho$ . In this case of digital images,  $\rho$  is a natural number, usually greater than or equal to 16.
- We define a new image called the local fractal dimension map, denoted by  $M$ , of the same size as  $I$ .
- For each pixel  $c = (x, y)$  in  $M$ , if  $x - \rho \geq 0$  and  $y - \rho \geq 0$  and  $x + \rho < w$  and  $y + \rho < h$  then we set the color of the pixel at  $(x, y)$  in  $M$  to  $\eta \circ \Phi_\rho(c)$ , where  $\Phi_\rho$  is the textural fractal dimension of the part of the image  $I$  inside (inclusively) the square  $(x - \rho, y + \rho) : (x + \rho, y + \rho)$  (the top-left corner : the bottom-right corner), i.e. the local fractal dimension in  $c$ .

The implementation is straightforward. All we have to do is to scan the original image and compute the local fractal dimension by using the gray-levels box-counting algorithm. However, one may notice that this is not an efficient solution as some of the computations are repeated. For instance, the maximum gray level inside a box, once computed in the procedure for the evaluation of the local fractal dimension in a pixel  $c$ , is computed again for all the pixels nearby  $c$ . Thus, it will take order of magnitudes longer times than necessary to compute the entire map and it will make the method impracticable in real-time applications. Given that in many situations, the local fractal dimension map is smooth enough, one can insert a parameter that makes the algorithm jump over the computation of some local fractal dimensions, i.e. the local fractal dimension will be computed only on a dense enough regular network of pixels of the image. These motivate the presentation of a much faster algorithm which takes the advantages of the observations:

#### OPTIMIZED ALGORITHM.

- Let  $I$  be a digital gray-levels image representing an object or a group of objects. Let  $w$  be the number of columns and  $h$  be the number of rows of pixels of the image. The columns and rows are indexed from 0.
- Let  $P$  be a fixed palette of colors, i.e. an array of  $(r, g, b)$  triples (red, green, blue) and  $\eta : [0, \infty) \rightarrow P$  be a function that associates a color to each non-negative real number.
- We fix the radius  $\rho$ . In this case of digital images,  $\rho$  is a natural number, usually greater than or equal to 16.
- We fix the “jumping” parameter  $\omega$ , a positive integer. Usually,  $\omega = \frac{\rho}{4}$  is a good choice.
- We fix the initial maximum size  $b_0$  of the boxes for the box counting method. This size must be smaller than  $\rho$  (usually it should be at least 4 times smaller).
- We generate the sequence  $J_{b_0}, J_{b_0-1}, \dots, J_0$  of images such that for all  $i \in \overline{0, b_0}$ ,  $J_i$  is an image with  $w - i$  columns and  $h - i$  rows indexed from 0, in the following way:
  - ◇  $J_0 = I$ .
  - ◇ For all  $i \in \overline{1, b_0}$  we put  $J_i(x, y) = \max\{I(x', y') : x \leq x' \leq x + i, y \leq y' \leq y + i\}$  for all  $0 \leq x < w - i$  and  $0 \leq y < h - i$ .
- We define a new image called the local fractal dimension map, denoted by  $M$ , of the same size as  $I$ .

- We compute the colors of the pixels in  $M$  in the following way:
  - ◊ For each pixel  $c = (x, y)$  in  $M$  with  $x \equiv 0 \pmod{\omega}$  and  $y \equiv 0 \pmod{\omega}$ , if  $x - \rho \geq 0$  and  $y - \rho \geq 0$  and  $x + \rho < w$  and  $y + \rho < h$  then we set the color of the pixel at  $(x, y)$  in  $M$  to  $\eta \circ \Phi_\rho(c)$ , where  $\Phi_\rho$  is the function that computes the textural fractal dimension of the part of the image  $I$  inside (inclusively) the square  $(x - \rho, y + \rho) : (x + \rho, y + \rho)$  (the top-left corner : the bottom-right corner), i.e. the local fractal dimension in  $c$ .
  - ◊ For the rest of the pixels  $c = (x, y)$  in  $M$  with  $x \not\equiv 0 \pmod{\omega}$  or  $y \not\equiv 0 \pmod{\omega}$  we set the color of the pixel at  $(x, y)$  in  $M$  to  $\eta \circ \Delta(c)$ , where  $\Delta(c)$  is the approximate value of the local fractal dimension in  $c$  obtained by the interpolation of the surrounding values computed by  $\Phi_\rho$ . The linear interpolation of nearby known values may be used. However, this step is not necessary if we set  $\omega = 1$ .

• The important thing is that the function  $\Phi_\rho$  has a different implementation in this algorithm than that of the previous version. Namely, each time we need to compute the maximum level of gray inside a box of size  $i \times i$ , with  $i \in \overline{0, b_0}$ , we get that value directly from  $J_i(x_0, y_0)$  where  $(x_0, y_0)$  is the top-left corner of the box.

**2.3. The graphical representation of the local fractal dimension map.** The local fractal dimension map  $\Phi_\rho$  (for a given  $\rho$ ) associates to each pixel of the given image, a local fractal dimension. Theoretically, for a gray-levels image, the map takes values up to 3.0, but computations can produce even higher values due to approximation errors. Therefore, we should reserve interpretations for all the real values in the interval  $[0, 4)$ . This interval is large enough for the task.

What we need is to represent the values of the map  $\Phi_\rho$ , for all the pixels of its domain, as a colored image on which the almost homogeneous areas will appear in almost the same color.

For this, we consider the standard *RGB* color model in which each pixel has a color represented as a triple  $(r, g, b)$  (red, green, blue), where each component of the triple takes an integer value between 0 and 255 so that the color space in the *RGB* color model can be represented as a 3-dimensional cube with the volume  $256^3$  and the *RGB* colors are the points on the  $\mathbb{Z}^3$  lattice inside the cube.

We consider two main ways to represent the local fractal dimension map:

(1) If we know the interval of possible values of the map for each type of structure in the image, then we may simply choose a different color for each interval. Moreover, if we want to visualize the fine structural differences on each of the structural homogeneous areas in the image, then we can map the interval of values characteristic to that type of structure to the different shades of the color assigned to that interval. We admit that the frontiers between structures give values of the local fractal dimension in different intervals than the intervals of the structures in contact. We associate different colors for these intervals associated to frontiers as well.

(2) In the second case, we suppose that we do not know any intervals of possible values of the local fractal dimension for the different structures in the image. Therefore, we need a method to visualize the structural differences in the image. The idea is to associate the colors to local fractal dimensions such that a small or big difference in colors denotes

a small or big difference in local fractal dimensions respectively. We propose a function which makes this association between fractal dimensions and colors and respects this criterion.

This function is  $C : [0, 4) \rightarrow \{0, \dots, 255\}^3$  with  $d \xrightarrow{C} (r, g, b)$  defined by

$$C(d) = (r(k(d)), g(k(d)), b(k(d)))$$

where  $k(d) = \lfloor 4000 * d \rfloor$  and

$$r(d) = 128 + \lfloor 126 * \sin(1\omega k(d) + 0.0) \rfloor$$

$$g(d) = 128 + \lfloor 126 * \sin(2\omega k(d) + 1.2) \rfloor$$

$$b(d) = 128 + \lfloor 126 * \sin(3\omega k(d) + 5.6) \rfloor$$

for some  $\omega$  that depends on how large is the variation of the local fractal dimension over the images in the studied set. Typical values are:  $\frac{\pi}{50}, \frac{\pi}{100}, \frac{\pi}{200}, \frac{\pi}{300}$ .

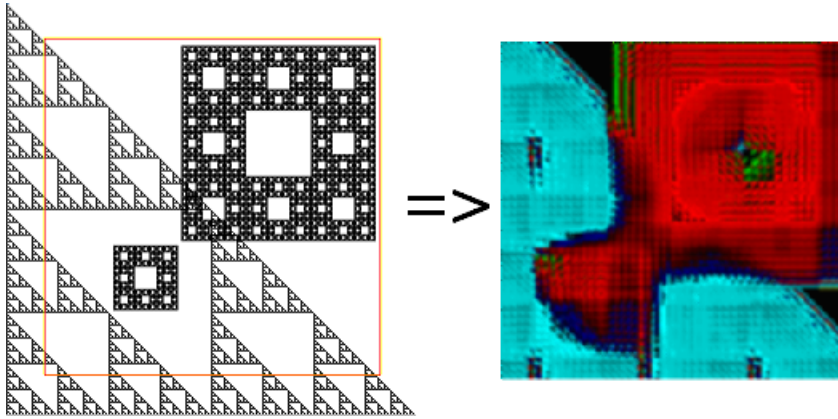


Fig. 3. A simple example of the Local Fractal Dimension Map computed for an image containing two types of structures (the Sierpiński Triangle and the Sierpiński Carpet). Different structures are represented by different colors by the map

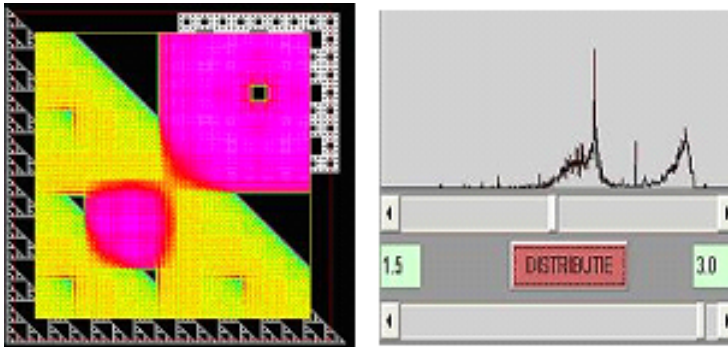


Fig. 4. A better representation of the Local Fractal Dimension Map (*left*) and the histogram of local fractal dimensions (*right*). The two strong peaks of the histogram correspond to the two dominant local fractal dimensions for the two structures respectively. The third narrow peak, in the middle, corresponds to the area in which the two structures overlap creating a third structure

In Fig. 3 and Fig. 4 we illustrate the local fractal dimension map of classical fractal structures while in Fig. 5 and Fig. 6 we illustrate the local fractal dimension map associated to some medical brain images [6].

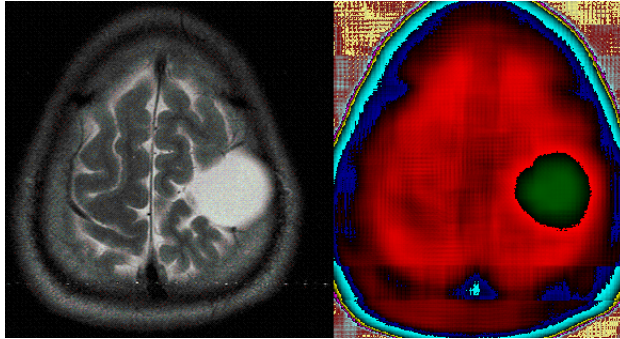


Fig. 5. The Local Fractal Dimension Map applied on the image of a brain with a tumor. The Local Fractal Dimension Map reveals a different tissue structure inside the healthy brain tissue structure

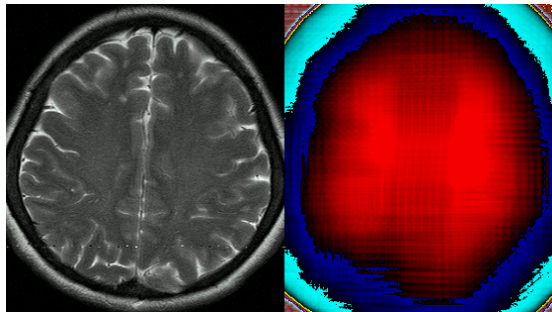


Fig. 6. The Local Fractal Dimension Map applied on the image of a healthy brain. The Local Fractal Dimension Map homogeneity inside the brain tissue reflects its structural homogeneity

**2.4. The frontier-band.** Suppose that the tumor is connected and is completely surrounded by the stroma. The classical notion of the frontier in this case is illustrated in Fig. 7.

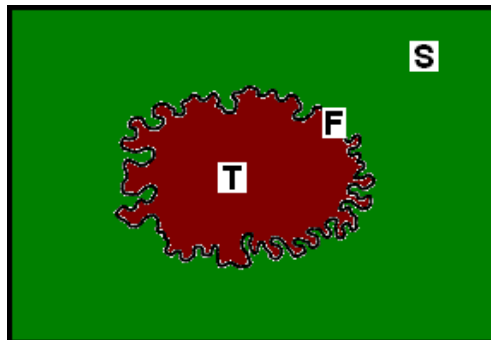


Fig. 7. The tumor-stroma frontier as it is classically viewed:  $T$ =tumor,  $S$ =stroma,  $F$ =frontier

This view ignores the interaction between the tumor and the stroma. More precisely, the tumor does not necessary look the same somewhere in the center as nearby the contact with the stroma where the interaction mostly takes place. The interaction between tumor and stroma plays an important role in the process of growth and therefore in the morphological features of the tumors. That is because not only the rule of growth of the tumor is different from the rule of growth of the stroma, but also the rule of growth of the tumor is affected by the interaction with stroma nearby at the contact zone and vice-versa [10, 4, 15]. One can imagine the rule of growth of the tumor cells combined in some way with the rule of growth of the stromal cells nearby the contact zone. Therefore, there are in fact three structures present in the image: a tumor structure, a stroma structure and a mixed structure where the interaction between tumor and stroma takes place. The notion of mixed structure, which does not lie on a curve (or surface embedded in the 3-dimensional space) but on an entire area (or volume in the 3-dimensional space), shall replace the notion of tumor-stroma frontier. What remains as classical frontiers is the boundary between the tumor and the mixed structure and the boundary between the stroma and the mixed structure respectively. We shall call the area on the image (or volume in the 3-dimensional space case) occupied by this mixed structure, the *frontier-band*.

This novel notion is illustrated in Fig. 8.

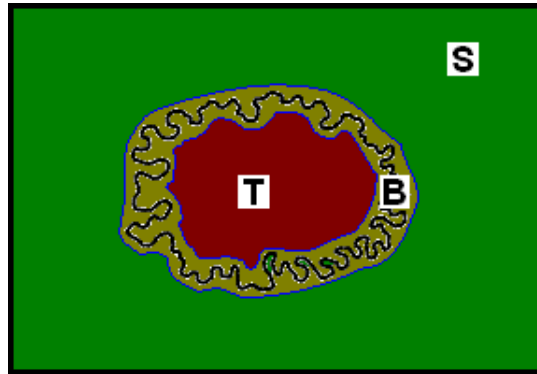


Fig. 8. The concept of tumor-stroma frontier-band:  $T$ =tumor,  $S$ =stroma,  $B$ =frontier-band

In the next subsection we describe how the frontier-band can be determined.

**2.5. Reconstruction of the frontier-band.** In the previous subsections we discussed how the local fractal dimension map  $\Phi_\rho$  is a way to investigate an object or a group of objects. The map  $\Phi_\rho$  tells the fractal dimension of every small part of the analyzed image. The size of the parts is determined by  $\rho$  and is related to the appropriate scale to evaluate the structural homogeneity in the given image.

The fractal dimension is an expression of the rule of growth. But the rule of growth is different on each of the three areas: inside the tumor, inside the stroma and on the frontier-band.

We choose  $\rho$  big enough such that the stroma will appear homogeneous enough on the map, but not bigger; the stroma is the structure we take as the reference for homogeneity.

In fact, the appropriate value of  $\rho$  probably reflects a measure of the cellular interaction inside the stroma (i.e. if the structural homogeneity only appears at a larger scale then perhaps the cellular interaction inside stroma manifests on larger distances).

The rule of interaction may be more complex than the rule of the tumor or the rule of stroma themselves, but the parameter  $\rho$  is chosen with respect to the structure of the stroma. Thus, the map may show heterogeneity on the frontier-band. But this is exactly what we shall exploit in order to evaluate the frontier-band. More precisely, we shall define the *frontier-band* as the heterogeneous area between the homogeneous area inside the tumor and the homogeneous area inside the stroma. Topologically, it looks like an annulus. This allows us to determine the frontier-band by using the local fractal dimension map. It is however possible that the entire tumor will be non-homogeneous with respect to the chosen parameters. In this case, the conclusions must take into account the particular medical context of the analysis.

There are at least two effective methods to determine the frontier-band accurately enough.

**METHOD 1.** The first method is applied when we know the two intervals of possible values of the local fractal dimensions of the small parts that belong to the interior of the tumor and to the interior of the stroma respectively. Suppose that the possible values of the map  $\Phi_\rho$  on the subdomain inside the stroma are known to belong to an interval  $[S_{\min}, S_{\max}]$ . Analogously, suppose that the possible values of the map  $\Phi_\rho$  on the subdomain inside the tumor are known to belong to an interval  $[T_{\min}, T_{\max}]$ . Suppose that  $T_{\max} < S_{\min}$ , the other case being analogous. Then, we shall define the frontier-band as the subdomain of the map  $\Phi_\rho$  on which its values lie inside the interval  $(T_{\max}, S_{\min})$ . See Fig. 9.

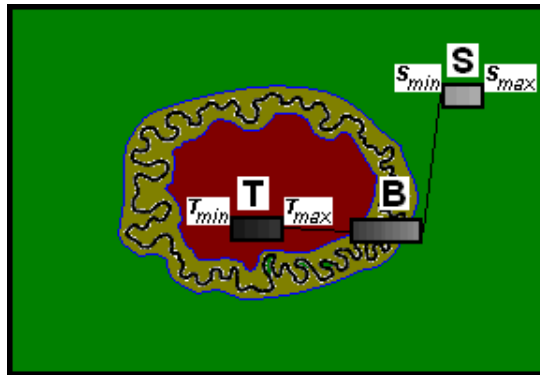


Fig. 9. Frontier-band identification method based on the prior knowledge of the local fractal dimensions intervals. The shades of gray represent different values of local fractal dimensions

**METHOD 2.** The second method is applied when we do not have any prior knowledge about the tumor tissue (i.e. no characteristic interval of possible local fractal dimensions is known for the tumor). In this case, we shall use the classical Region-Growing segmentation method applied on the local fractal dimension map and not on the original image.

The seed pixels can be chosen in different ways, depending on the information we have about the tumor. However, we present below two simple and general algorithms for choosing the seed pixels:

(1) The first method is to choose the seed pixels as the pixels inside a discrete disk subdomain  $D$  on the map  $\Phi_\rho$ , such that  $D$  is approximately equally distanced from the stroma border. The size of the disk  $D$  should be chosen in such a way that another disk with a double radius could fit inside the subdomain delimited by the border of the stroma (see Fig. 10).

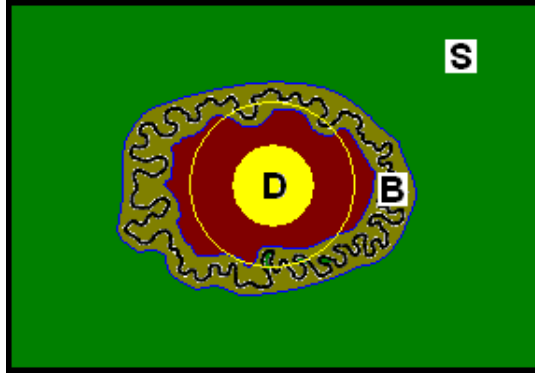


Fig. 10. Frontier-band identification method based on the Region-Growing method applied on the local fractal dimension map by using the seed pixels in the disc  $D$

(2) The second method is to choose the seed pixels as the pixels inside a subdomain  $K$  obtained by the repeated application of the erosion morphological operator on the subdomain delimited by the border of the stroma (see Fig. 11).

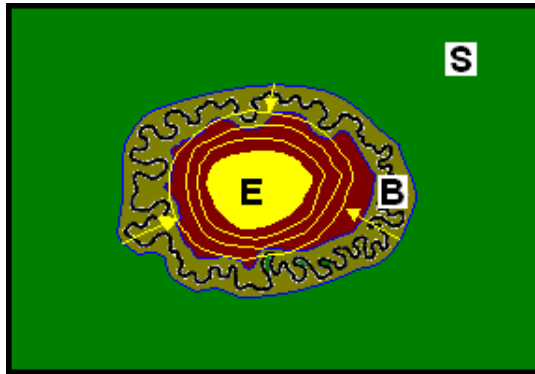


Fig. 11. Frontier-band identification method based on the Region-Growing method applied on the local fractal dimension map by using the seed pixels in the eroded shape  $E$

**2.6. Frontier-band analysis.** The local fractal dimension map is smooth enough to make inappropriate any evaluation of the fractal dimension of contour lines. Therefore, only the spatial distribution of its values over the domain counts as a criterion. We present below some criteria for the evaluation of the frontier-band proven to be very efficient in applications.

**2.6.1. The area of the frontier-band and the  $\mathbb{I}$ -Index.** The area of the domain occupied by the frontier-band is one important criterion. It is a substitute of the fractal dimension of the contour of the tumor which will not be dependent on the color-based segmentation algorithm. By the definition of the frontier-band, if this area is larger, then it means that the tumor and the stroma interact on a larger domain.

One can compare this area with the area of the domain occupied by the interior of the tumor to obtain an absolute index for comparisons which reflects the interaction between the tumor and the stroma. We shall call this index the *Interlacement Index* or  $\mathbb{I}$ -Index.

DEFINITION 6. Let  $\Phi_\rho$  be the local fractal dimension map associated to an image of a tumor inside a stroma. Let  $T$  denote the domain occupied by the tumor,  $S$  denote the domain occupied by the stroma and  $F$  denote the domain occupied by the frontier-band. Let  $A_T$  denote the area occupied by the interior of the tumor and let  $A_F$  denote the area occupied by the frontier-band. Then we define the  $\mathbb{I}$ -Index as

$$\mathbb{I}_\rho(T, F, S) = \frac{\sqrt{A_T + A_F} - \sqrt{A_T}}{|\mathcal{F}_T - \mathcal{F}_S|}$$

where  $\mathcal{F}_T$  is the mean local fractal dimension of the tumor tissue and  $\mathcal{F}_S$  is the mean local fractal dimension of the stroma tissue.

*Justification.* If we reduce the interior of the tumor, the frontier-band and the interior of the stroma to their simplest form, then we can represent them as in Fig. 12.

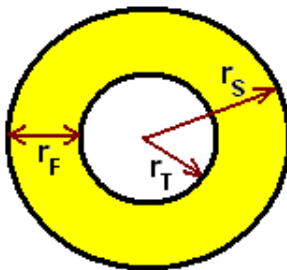


Fig. 12. The idealized form of *Tumor — Frontier-Band — Stroma*

We are interested in the difference  $r_F = r_S - r_T$ . Since  $A_T = \pi r_T^2$ , it follows that  $r_T = \sqrt{A_T/\pi}$ . Similarly, since  $A_T + A_F = \pi r_S^2$ , it follows that  $r_S = \sqrt{(A_T + A_F)/\pi}$ . Thus,  $r_F = (\sqrt{A_T + A_F} - \sqrt{A_T})/\sqrt{\pi}$ . Discarding the constant  $1/\sqrt{\pi}$  and normalizing the result by the difference between the fractal dimensions of the two regions, we obtain the Interlacement Index  $\mathbb{I}_\rho(T, F, S)$ .

**2.6.2. The radial homogeneity of the frontier-band and the  $\mathbb{RH}$ -Index.** Another criterion for the evaluation of the frontier-band is the radial homogeneity. By radial homogeneity we understand the homogeneity of the distribution profile of the values of the map  $\Phi_\rho$  over the frontier-band when we evaluate it along the transverse segments from the border of the interior of the tumor to the border of the interior of the stroma. The variation of the profiles along the frontier-band gives a new index called the *Radial Homogeneity Index* or  $\mathbb{RH}$ -Index.

DEFINITION 7. Let  $\Phi_\rho$  be the local fractal dimension map associated to an image of a tumor inside a stroma. Let  $T$  denote the domain occupied by the tumor,  $S$  denote the domain occupied by the stroma and  $F$  denote the domain occupied by the frontier-band. For any pixel  $p$  on the border of  $S$ , we denote by  $q_p$  the closest pixel to  $p$  on the border of  $T$ . The discrete segment  $C_p = [p, q_p]$  is called the *transverse* from  $p$ . The restriction  $\Phi_\rho|_{C_p}$  is called the *profile* on the transverse  $C_p$ .

Let  $E$  be any real valued function that evaluates the profile of a transverse, called the *profile evaluation function*. One may take  $E$  to be simply the length of the transverse.

For a chosen profile evaluation function  $E$ , we define the radial homogeneity index of the frontier-band as the dispersion of the values of  $E$  along the border of  $S$  (see Fig. 13).

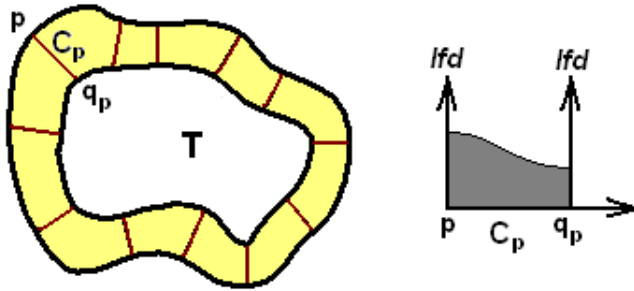


Fig. 13. The transverse segments of the frontier-band (*left*) and an example of a distribution profile along a transverse segment (*right*)

**3. Applications.** The frontier-band analysis can be applied in the different instances of medical image analysis: brain tumors, liver tumors, skin tumors etc. However, different classes of tumors require particular statistical studies and algorithms to effectively use the construction of the frontier-band. For instance, the construction of the frontier-band has been successfully applied in the case of skin moles analysis (adapted to this class of tumors), together with particular algorithms dedicated to skin moles in a smart-phones application for which the analysis algorithm have been developed by the author. Although the algorithms themselves cannot be presented here, they are based on the local fractal dimension map and the notion of frontier-band. The moles are classified by this application as “low risk”, “medium risk” or “high risk” according to the results of the image analysis. The results have been compared to the opinion of three specialists. On a hand-camera (8Mpx), the classification have been up to 90% accurate on a test set of about 70 images. On a mobile phone camera (5Mpx), the classifications have been up to 70+ percents accurate on the set of about 50000 images received from the users [12].

**4. Conclusions.** We described the construction of the local fractal dimension map for a given image and we presented two algorithms for its computation, the basic one and an enhanced one applicable in real-time. The local fractal dimension map is a tool which helps to identify the different biological structures in a medical image. The areas occupied by the different structures (e.g. tumor or stroma) on the image will appear in different

colors on the graphical representation of the local fractal dimension map. The local fractal dimension map allows us to define the tumor-stroma frontier as a band instead of a curve and makes possible the fractal analysis of the interaction between the tumor and the stroma without appealing to any form of non-fractal analysis along the way. We described the construction procedure of the frontier-band for a given tumor-stroma image. For the analysis of the frontier-band, we defined two numbers called  $\mathbb{I}$ -Index and  $\mathbb{RH}$ -Index respectively which characterize the tumor-stroma interaction. The analysis of the frontier-band can be applied in many contexts in which the frontier is relevant. For instance, the frontier-band analysis has been successfully used by the author in developing accurate analysis algorithms for skin lesion. Recently, these algorithms were evaluated in a clinical study performed at the University of Munich in Germany and published in [5].

**Acknowledgments.** The research presented in this article was partially supported by Politehnica University of Bucharest through the project POSDRU/88/1.5/S/60203 and represent a part of the work developed by the author in his PhD thesis *Fractal analysis and cellular automata modeling of biological growth processes* (Bucharest, 2012).

### References

- [1] N. A. Bhowmick, E. G. Neilson, H. L. Moses, *Stromal fibroblasts in cancer initiation and progression*, Nature 432 (2004), 332–337.
- [2] R. C. Gonzalez, R. E. Woods, *Digital Image Processing*, second ed., Prentice Hall, New Jersey 2002.
- [3] R. Kalluri, M. Zeisberg, *Fibroblasts in cancer*, Nat. Rev. Cancer 6 (2006), 392–401.
- [4] Y. Kitadai, *Cancer-stromal cell interaction and tumor angiogenesis in gastric cancer*, Cancer Microenvironment 3 (2010), 109–116.
- [5] T. Maier et al., *Accuracy of a smartphone application using fractal image analysis of pigmented moles compared to clinical diagnosis and histological result*, in: Journal of the European Academy of Dermatology and Venereology 29 (2015), 663–667.
- [6] M. Olteanu, R. Dragomir, M. Tanase, *The analysis of CT and MR brain images using box-counting-type methods*, in: Interdisciplinary Approaches in Fractal Analysis, Bucharest 2003, 267–273.
- [7] T. Pavlidis, *Algorithms for Graphics and Image Processing*, Springer, Berlin 1982.
- [8] H. O. Peitgen, H. Jürgens, D. Saupe, *Chaos and Fractals: New Frontiers of Science*, Springer, New York 1992.
- [9] M. Petrou, P. Bostdogianni, *Image Processing: the Fundamentals*, Wiley, UK 2004.
- [10] K. Polyak, R. Kalluri, *The role of the microenvironment in mammary gland development and cancer*, Cold Spring Harbor Perspectives in Biology 2 (2010), art. a003244.
- [11] D. Popescu, M. Nicolae, D. A. Crisan, N. Angelescu, *Computer aided diagnosis in mammography based on fractal analysis*, in: Proc. of the 5th WSEAS Int. Conf. on Non-Linear Analysis, Non-Linear Systems and Chaos, Bucharest 2006.
- [12] M. Tanase, *Fractal analysis and cellular automata modeling of biological growth processes*, PhD Thesis, Politehnica University of Bucharest, 2012.

- [13] M. Tanase, R. Dobrescu, *Fractal analysis of growth processes modeled by using cellular automata mixes*, in: *Fractals and Complexity*, ed. P. Waliszewski, Wrocław, FA Format, 2013, ISBN 978-83-936598-0-7, 24–30. (The work was presented to the 8th European Congress of Mathematical and Theoretical Biology, Cracow, Poland, 2011.)
- [14] C. Vasilescu, V. Herlea, F. Talos, B. Ivanov, R. Dobrescu, *Differences between intestinal and diffuse type of gastric carcinoma: a fractal analysis*, in: *Interdisciplinary Applications of Fractal and Chaos Theory*, eds. R. Dobrescu, C. Vasilescu, Romanian Academy Ed., Bucharest 2004, 247–254.
- [15] T. L. Whiteside, *The tumor microenvironment and its role in promoting tumor growth*, *Oncogene* 27 (2008), 5904–5912.